Proceedings of the ASME 32th International Conference on Ocean, Offshore and Arctic Engineering
OMAE2013
June 9-14, 2013, Nantes, France

OMAE2013-10156

JOINT ENVIRONMENTAL DATA AT FIVE EUROPEAN OFFSHORE SITES FOR DESIGN OF COMBINED WIND AND WAVE ENERGY DEVICES

Lin Li, Zhen Gao, Torgeir Moan
Centre for Ships and Ocean Structures (CeSOS)
Norwegian University of Science and Technology(NTNU)
Otto Nielsens vei 10, NO-7491, Trondheim, Norway
Emails: lin.li@ntnu.no; zhen.gao@ntnu.no; torgeir.moan@ntnu.no

ABSTRACT

The costs for an offshore wind farm, especially with bottom fixed foundations increase significantly with increasing water depth. If costs can be reduced to a competitive level, the potential for wind farms in deep water is huge. One way of reducing costs might be to combine offshore wind with wave energy facilities at sites where these resources are concentrated.

In order to design combined renewable energy concepts, it is important to choose sites where both wind and wave energy resources are substantial. Such facilities might be designed in ultimate limit states based on load effects corresponding to 50-year wind and wave conditions. This requires a long-term joint probabilistic model for the wind and wave parameters at potential sites.

In this paper, five European offshore sites are selected for analysis and comparison of combined renewable energy concepts developed in the EU FP7 project – MARINA Platform. The five sites cover both shallow water (<100m) and deep water (>200m), with three sites facing the Atlantic Ocean and the other two sites in the North Sea. The selection of the sites is carried out by considering average wind and wave energy resources, as well as extreme environmental conditions which indicate the cost of the system.

Long-term joint distributions of mean wind speed at 10-meter height (U_w), significant wave height (H_s) and spectral peak period (T_p) are presented for selected sites. Simultaneous hourly wind and wave hindcast data from 2001-2010 are used as a database, which are obtained from the National and Kapodistrian University of Athens.

The joint distributions are estimated by fitting analytical distributions to the hindcast data following a procedure suggested by Johannessen et al. (2001). The long-term joint distributions can be used to estimate the wind and wave power output from each combined concept, and to estimate the fatigue lifetime of the structure. For estimation of the wind and wave power separately, the marginal distributions of wind and wave are also provided.

Based on the joint distributions, contour surfaces are established for combined wind and wave parameters for which the probability of exceedance corresponds to a return period of 50 years. The design points on the 50-year contour surfaces are suggested for extreme response analysis of combined concepts. The analytical long-term distributions established could also be applied for design analysis of other offshore structures with similar environmental considerations of these sites.

INTRODUCTION

Offshore wind has an enormous potential for a long-term sustainable energy supply. However, as the installed capacity increases, suitable sites in shallow waters are becoming scarce – driving the technology into deeper waters. The exploitation of deeper waters comes with significant design, installation, grid connection, operation and maintenance challenges, which will increase the costs significantly. One possible way of reducing offshore wind costs is to exploit synergies with other renewable marine technologies. One choice is to combine offshore wind with wave energy at sites where both resources are concentrated. The EU project – MARINA Platform is dedicated to investigate the potential for combining offshore wind and wave energy devices [1]. Many new concepts with combinations of different wind turbines and wave energy converters are under analysis in this project.

For design of these combined concepts, 50-year extreme responses should be examined [2]. A consistent approach is to estimate the full long-term responses, in which the responses at all of the environmental conditions should be taken into account with the consideration of their probability of occurrence, so it requires a large number of simulations. For a complicated response problem, the computational time is rather long, which makes the full long-term analysis impractical.

In this case, it is more convenient to apply the contour surface method (contour line method when two environmental variables are present) [3,4] to estimate the long-term extremes by exposing the structure to a short-term extreme sea state. Several sea states are chosen from the 50-year environmental contour surfaces, which can be extrapolated from a long-term joint distribution. The sea states that leads to the largest response should be chosen as the designed sea states. To account for the variability of the sea states, one derived extreme value needs to be taken considering a higher quantile of 75%-90% [5] rather than 50%. Alternatively, it can be obtained by multiplying a correction factor of 1.1-1.3 [6].

Therefore, in order to predict estimates for the 50-year response extremes, one in principle needs a long-term joint distribution model of important environmental parameters under consideration. Johannessen et al. [7] described a procedure to achieve joint distributions of wind and wave parameters and presented contour surfaces at one location in the Northern North Sea. To compare and analyse different combined wind and wave concepts, environmental information at more sites located at different areas should be applied.

The purpose of this paper is to provide a set of environmental conditions for the design of combined concepts. Five sites in both the Atlantic Ocean area and the North Sea area are considered. The sites are selected by comparing the factors indicating the energy outputs and the costs of the concepts. Long-term joint distributions of mean wind speed at 10-meter height (U_w), significant wave height (H_s) and spectral peak period (T_p) at these sites are acquired by fitting 10 years' environmental hindcast data by using the procedure described by Johannessen et al [7]. For conditional distribution of T_p for given U_w and H_s, a simplified method is discussed. It is shown that the simplified method does not influence the determination of critical conditions for design purpose. Finally, the 50-year contour surfaces at the five sites are presented for the extreme response analysis.

ENVIROMENTAL CONDITIONS AT FIVE SELECTED EUROPEAN OFFSHORE SITES

Data description

The environmental data used in this study are generated by a numerical hindcast model from National and Kapodistrian University of Athens (NKUA). In order to select proper sites for the combined wind and wave energy concepts, a large database is needed for comparisons of site conditions, and observations can hardly satisfy the requirements. Hence, numerical hindcast data are more appropriate than observational records for site selection due to its wide spatial and temporal coverage and homogeneity.

The wave model uses wind input produced by the atmospheric model and the grid of the wave model covers the whole North Atlantic Ocean [8]. Assimilation techniques are applied for the correction of initial wind and wave conditions [9,10]. By comparing with measurements, the results from the numerical model are generally correlated to the measurements. However, the numerical model has some uncertainties in cases of shallow water or mixed seas (swell and wind sea), which require more calibrations [11].

Selection of European sites

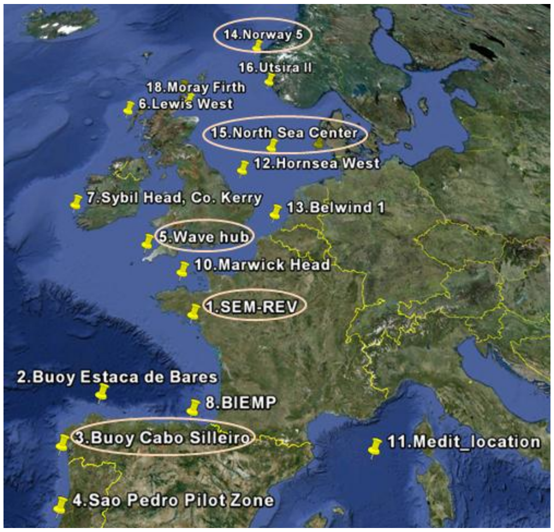

FIGURE 1. LOCATION OF EIGHTEEN POTENTIAL EUROPEAN OFFSHORE SITES

Eighteen sites in the Atlantic Ocean and the North Sea area are considered as potential sites for the design of combined renewable energy concepts in the MARINA Platform project. General information and important statistics of these sites are shown in Table 1. The locations of these sites are pin-pointed on the map in Figure 1. Based on the information in the table, we can observe some characteristics of these sites:

1) The average water depth in the North Sea area is relatively small except for the sites close to Norway (site 14 and 16). For some of the sites which are very far from shore (site 15) the water depth are still very small. However, there exists a variation in water depth in the North Sea area. These sites with shallow water depth are suitable for bottom-fixed concepts.

2) Sites at Atlantic area have more wave energy resources on average compared to those at the North Sea area while the wind resources vary less from area to area except for sites 6, 7, 14 and 16 for which the available wind power is larger.

3) Two types of wave period distribution are envisaged. The average T_p in the Atlantic Ocean is larger than that in the North Sea area. One important reason is that the area is relatively open in the Atlantic Ocean, so swell occurs more frequently which contributes to the large T_p value while the waves in the North Sea area are mainly wind-generated waves, except for site 14 and 16 in the Northern North Sea which are actually open to the Atlantic Ocean.

TABLE 1. GENERAL INFORMATION AND STATICS OF EIGTEEN EUROPEAN OFFSHORE SITES

Site No.	Area	Name	Water depth (m)	Distance to shore (km)	Average wind power density at 80m height (W/m^2)	Average wave power density (kW/m)	50-year mean wind speed at 10m height (m/s)*	50-year significant wave height (m)*	Mean value of T_p (s)
01	**Atlantic**	**Sem Rev**	**33**	**15**	**530.31**	**16.51**	**23.76**	**8.15**	**11.06**
02	Atlantic	Buoy Estaca de Bares	694	30	691.04	46.73	27.87	10.67	11.66
03	**Atlantic**	**Buoy Cabo Silleiro**	**449**	**40**	**647.72**	**42.72**	**28.37**	**10.19**	**11.84**
04	Atlantic	Sao Pedro Pilot Zone	60	20	356.19	32.47	23.62	8.32	11.73
05	**Atlantic**	**Wave Hub**	**43**	**20**	**620.75**	**31.79**	**27.46**	**10.22**	**11.26**
06	Atlantic	Lewis West	43	25	1121.92	65.16	30.66	12.71	11.70
07	Atlantic	Sybil Head, Co. Kerry	103	20	946.20	70.36	29.50	13.37	11.77
08	Atlantic	BIMEP	1	3	193.80	37.1	24.44	12.68	11.89
09	Atlantic	EMEC Wave West Buoy	24	3	647.42	37.86	32.24	11.84	11.68
10	English Channel	Marwick Head	68	20	660.28	28.38	26.58	9.32	11.17
11	Mediterranean	Mediterranean location	2558	150	739.81	12.56	34.76	12.45	5.87
12	North Sea	Horn Sea West	42	50	805.84	9.29	26.69	7.02	6.81
13	North Sea	Belwind 1	31	40	754.19	6.04	26.81	6.54	5.55
14	**North Sea**	**Norway 5**	**202**	**30**	**1094.84**	**46.43**	**33.49**	**10.96**	**11.06**
15	**North Sea**	**North Sea Center**	**29**	**300**	**871.03**	**14.29**	**27.20**	**8.66**	**6.93**
16	North Sea	Utsira II	277	20	913.94	28.68	32.45	10.11	10.05
17	North Sea	FINO 3	22	60	850.95	12.79	26.49	8.62	6.70
18	North Sea	Moray Firth	46	25	659.87	6.05	26.50	5.94	6.77

* The 50-year mean wind speed at 10m height and the 50-year significant wave height are obtained from the marginal distributions.

After a study on the environmental data at these eighteen sites, it is noted that some of the sites have very similar wind and wave conditions. Therefore, it is concluded that five of these eighteen sites are representative for concept comparison of the combined wind and wave energy concepts. The following three important factors are considered for site selection:

1) Site geographic conditions (area, water depth and distance to shore);
2) Average wind and wave energy resources;
3) Extreme values of wind and wave conditions.

First, the selected sites should cover both Atlantic Ocean and the North Sea area, and include both deep water and shallow water for bottom-fixed and floating concepts respectively. Then, for combined wind and wave energy concepts, it is essential to require the specified sites to have both considerable wind and wave energy resources. Finally, the extreme wind speeds and significant wave heights should be examined to avoid significant increase to the costs.

Table 1 lists the factors mentioned above for the eighteen potential sites. For wind energy resources, wind power at 80 meters level which is the hub height of a typical offshore wind turbine is calculated. The average available wind and wave power density are the mean value of the power density at each hour in the 10 years' duration calculated from Eq. (1) based on the deep water assumption.

$$P_{wind} = \frac{\rho_{air}}{2} U_{80}{}^{3}, \quad P_{wave} = \frac{\rho_{water} g^{2}}{64\pi} H_S{}^{2} T_E \qquad (1)$$

where U_{80} is the wind speed at 80m height; H_s is the significant wave height; and T_E is the wave energy period given by

$$T_E = \frac{2\pi}{\omega_E} = 2\pi \frac{m_{-1}}{m_0}, \quad m_k = \int_0^{\infty} \omega^k S(\omega) d\omega \qquad (2)$$

Where m_{-1} and m_0 are the minus one and zero spectral moments; and $S(\omega)$ is the wave spectrum.

The 50-year extreme values of wind speed and significant wave height in Table 1 are obtained by extrapolation of the marginal distributions of wind speed at 10 meters level and significant wave height. Two-parameter Weibull distributions are applied for both distributions. It will be shown later that Weibull distribution does not fit the marginal distribution of H_s perfectly for some sites and will underestimate the extreme values. However, in site selection process only two-parameter Weibull distribution is applied for simplicity. Other fitting methods will be introduced in the next section.

By considering the factors mentioned above, five sites are finally selected which are marked in Figure 1, with site information presented in Table 1. Moreover, a generic water depth (40m, 100m and 200m) will be considered instead of the actual water depth at each site for concept design. The site conditions are:

1) Site No. 01 with water depth of 40m
2) Site No. 05 with water depth of 40m
3) Site No. 15 with water depth of 40m
4) Site No. 03 with water depth of 200m
5) Site No. 14 with water depth of 100m and 200m

In the MARINA Platform project, analyses will be carried out at Site No. 01, 05 and 15 for bottom-fixed combined concepts, while for floating concepts analyses will be carried out at Site No. 03 and 14.

PREDICTION OF LONG-TERM ENVIRONMENTAL CONDITIONS

The hindcast data has been sampled hourly for wind and wave and archived in a database from 2001 to 2010. The parameters used in the long-term joint distributions are:

- Mean wind speed at 10 meters height, U_w
- Significant wave height, H_s
- Wave spectral peak period, T_p

Marginal and joint distributions of wind and wave conditions are acquired by fitting analytical distributions to the raw data. The joint distribution of U_w, H_s and T_p can be applied to estimate the power output from the wind turbines and the wave energy converters in a combined concept. It should be noted that the mean wind speed considered in the joint distribution is at the height of 10 meters above the sea level. For power estimation of wind turbines, the mean wind speed at hub height is needed (e.g. the hub height of NREL 5MW wind turbine is 89m above the sea level) and can be obtained considering a wind speed profile. A preliminary study on wind speed at different levels indicates that a power law profile with the exponent α equal to 0.1 can be used for all of the five sites.

$$U(z) = U_{10}\left(\frac{z}{10}\right)^{\alpha} \quad (3)$$

where z represents the height, U_{10} is the mean wind speed at the reference height of 10 meters.

Usually it is more precise to use wind speed at higher levels if the wind profile is not stable. However, the wind speeds at all heights in the rotor plane (e.g from 10m to 180m) of a wind turbine need to be considered for wind turbine load and response analysis. Therefore, for simplicity in present study the reference mean wind speeds at 10m height and a constant wind speed profile parameter α = 0.1 are used to estimate wind speeds at higher levels.

For the case the wind and wave power is estimated separately, the marginal distributions of wind and wave are provided. The marginal distribution of U_w (at hub height) can be used to estimate the wind power given the power curve of the wind turbine. Similarly, the joint distribution of H_s and T_p can be utilized to estimate the wave power given the power matrix of the wave energy converter.

As for ultimate limit state analysis, the environmental contour surface with a return period of 50 years is obtained. Extreme conditions with combinations of U_w, H_s and T_p can be selected along the contour surface.

Long-term distributions of wind and wave directions are not considered in this study and it is assumed that wind and waves are collinear and always have the same direction.

The fitting methods of marginal and joint distributions will be explained in details in the following subsections, and figures illustrating the fitting results at Site 14 are presented as examples to show the goodness of the fittings.

Marginal distribution of mean wind speed U_w

The raw data at five selected sites indicate that one-hour mean wind speed at 10m height (U_w) follows a two-parameter Weibull distribution and the probability density function is given in Eq. (4). Figure 2 shows the fitting curve of marginal distribution of U_w at Site 14 on the Weibull probability paper. A good agreement between the raw data and the fitting is obtained. It should be mentioned that the maximum likelihood method is applied for the fittings of the distributions in this paper.

$$f_{Uw}(u) = \frac{\alpha_U}{\beta_U}\left(\frac{u}{\beta_U}\right)^{\alpha_U - 1} \exp\left[-\left(\frac{u}{\beta_U}\right)^{\alpha_U}\right] \quad (4)$$

α_U and β_U denote the shape and scale parameters, respectively. In this paper, $f()$ refers to the probability density function (PDF).

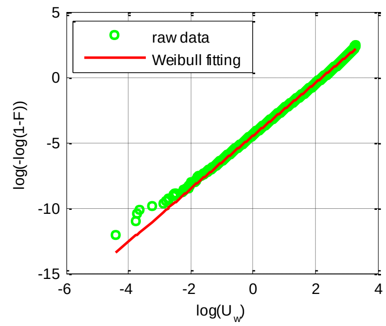

FIGURE 2. WEIBULL PLOT OF MARGINAL DISTRIBUTION OF U_w AT SITE 14

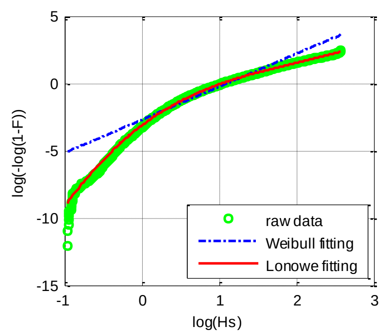

FIGURE 3. WEIBULL PLOT OF MARGINAL DISTRIBUTION OF H_s AT SITE 14 (h_0=5.0m)

Joint distribution of H_s and T_p

If only the wave data are considered, a joint PDF of H_s and T_p can be established. It consists of a marginal distribution of H_s and a conditional distribution of T_p for given H_s.

$$f_{Hs,Tp}(h,t) = f_{Hs}(h) \cdot f_{Tp|Hs}(t|h) \quad (5)$$

Regarding the marginal distribution of H_s, it seems that the main part of raw data follow a lognormal distribution while the data in the tail follow a Weibull distribution. Therefore, the hybrid lognormal and Weibull distribution - Lonowe model developed by Haver [12] is applied and the PDF is shown in Eq. (6).

$$f_{Hs}(h)=\begin{cases}\dfrac{1}{\sqrt{2\pi}\sigma_{LHM}h}\exp\left(-\dfrac{1}{2}\left(\dfrac{\ln(h)-\mu_{LHM}}{\sigma_{LHM}}\right)^2\right) & h\le h_0\\ \dfrac{\alpha_{HM}}{\beta_{HM}}\left(\dfrac{h}{\beta_{HM}}\right)^{\alpha_{HM}-1}\exp\left[-\left(\dfrac{h}{\beta_{HM}}\right)^{\alpha_{HM}}\right] & h>h_0\end{cases} \qquad (6)$$

h_0 is the shifting point of H_s from the lognormal distribution to the Weibull distribution. μ_{LHM} and σ_{LHM} are the parameters in the lognormal distribution, i.e. the mean value and the standard deviation of ln(h), the natural logarithm function of h. α_{HM} and β_{HM} are the shape and scale parameters in the Weibull distribution, which are calculated by using the continuity condition of probability density function and cumulative density function at the shifting point. Figure 3 shows the fitting results of marginal distribution of H_s from a Lonowe model at site 14 on the Weibull probability paper. The fitted line from a pure Weibull model is also shown for comparison and this model does not fit the whole range of the data well from the figure.

For conditional distribution of T_p for given H_s, the data seem to follow a lognormal distribution, which is also suggested by Johannessen et al [7].

$$f_{Tp|Hs}(t|h)=\frac{1}{\sqrt{2\pi}\sigma_{LTC}t}\exp\left(-\frac{1}{2}\left(\frac{\ln(t)-\mu_{LTC}}{\sigma_{LTC}}\right)^2\right) \qquad (7)$$

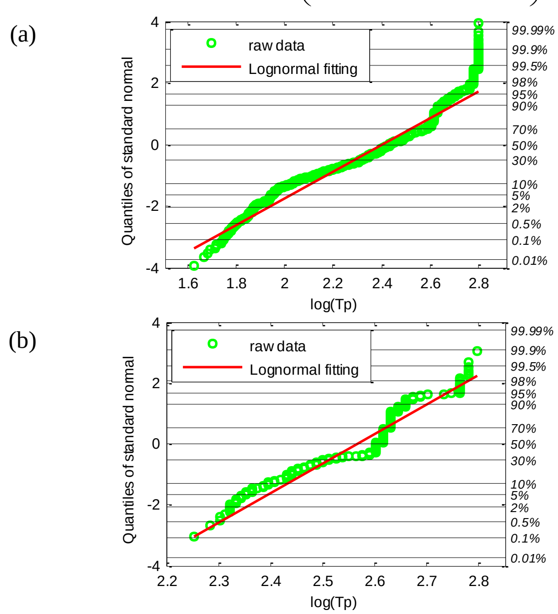

FIGURE 4. LOGNORMAL PLOT OF CONDITIONAL DISTRIBUTION OF T_p FOR GIVEN H_s AT SITE 14 (a. 2.5m<H_s<3.0m; b. 7.0m<H_s<7.5m)

The conditional distribution of T_p is estimated for different H_s classes with a bin size of 0.5m. Figure 4 shows the lognormal distribution fitting curves of T_p at two H_s classes. It can be seen that the lognormal distribution are reasonable for both low and high wind classes. In order to describe the conditionality of T_p on H_s, the mean value μ_{LTC} and variance σ^2_{LTC} of ln(t) are formed by smooth functions of H_s:

$$\mu_{LTC}=c_1+c_2h^{c_3} \qquad (8)$$

$$\sigma^2_{LTC}=d_1+d_2\exp(d_3h) \qquad (9)$$

where exp( ) represents the exponential function. c_1, c_2, c_3, d_1, d_2 and d_3 are the parameters estimated from the raw data by nonlinear least-square curve fitting. The fittings are shown in Figure 5.

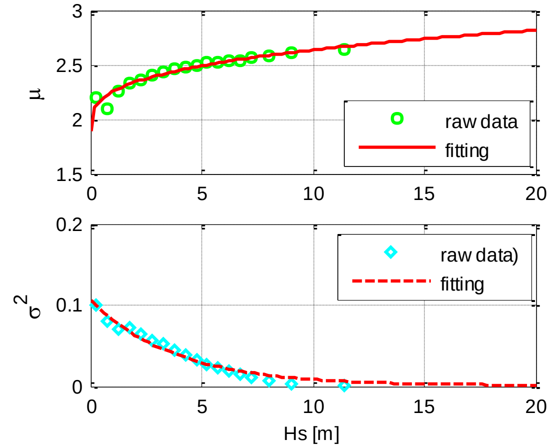

FIGURE 5. FITTING OF LOGNORMAL PARAMETERS OF CONDITIONAL DISTRIBUTION OF T_P FOR GIVEN H_s (SITE 14)

Joint distribution of U_w, H_s and T_p

The joint distribution of U_w, H_s and T_p consists of a marginal distribution of U_w, a conditional distribution of H_s for given U_w and a conditional distribution of T_p for given both U_w and H_s.

$$f_{Uw,Hs,Tp}(u,h,t)=f_{Uw}(u)\cdot f_{Hs|Uw}(h|u)\cdot f_{Tp|Uw,Hs}(t|u,h) \qquad (10)$$

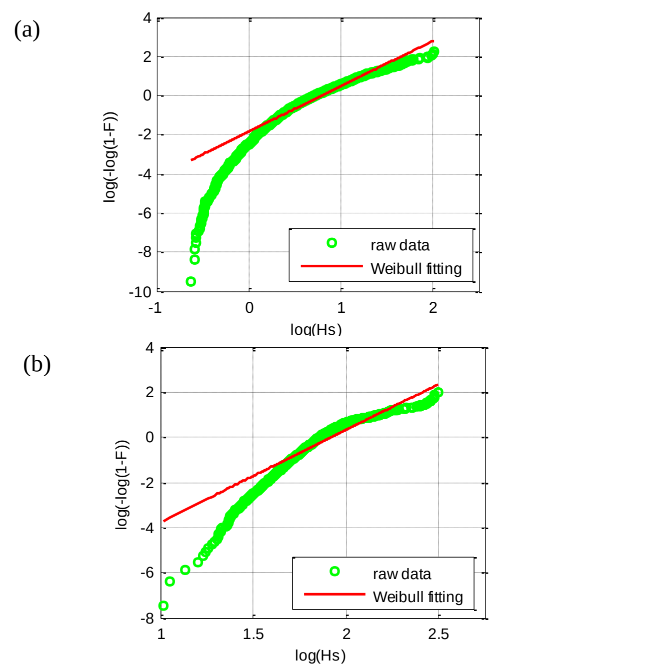

FIGURE 6. WEIBULL PLOT OF CONDITIONAL DISTRIBUTION OF H_s FOR GIVEN U_w AT SITE 14 (a. 4.0m<U_w<5.0m; b. 19.0m<U_w<20.0m)

The marginal PDF of U_w is the same as Eq. (4), while the conditional PDF of H_s is given as two-parameter Weibull distribution,

$$f_{Hs|Uw}\left(h|u\right)=\frac{\alpha_{HC}}{\beta_{HC}}\left(\frac{h}{\beta_{HC}}\right)^{\alpha_{HC}-1}\exp\left[-\left(\frac{h}{\beta_{HC}}\right)^{\alpha_{HC}}\right] \qquad (11)$$

where α_{HC} and β_{HC} are the shape and scale parameters, respectively.

Figure 6 shows two examples of fitting curves of H_s at two U_w classes. The bin size of the wind data is 1m/s. It seems that the raw data in low wind speed classes indicate a Lonowe model for conditional H_s distribution, while for high wind speeds a Weibull model is more suitable. To get more accurate fitting for H_s at high wind classes, only the Weibull model is considered. The shape and scale parameters are fitted as power functions of mean wind speed to express the conditionality:

$$\alpha_{HC}=a_1+a_2u^{a_3} \qquad (12)$$

$$\beta_{HC}=b_1+b_2u^{b_3} \qquad (13)$$

where a_1, a_2, a_3, b_1, b_2 and b_3 are the parameters estimated from the raw data by nonlinear curve fitting and the fitting curves are shown in Figure 7.

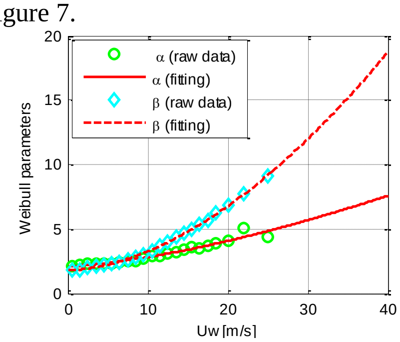

FIGURE 7. FITTING OF WEIBULL PARAMETERS OF CONDITIONAL DISTRIBUTION OF *Hs* FOR GIVEN *Uw* (SITE 14)

For the conditional distribution of T_p for given H_s and U_w, the data in each wind-wave class indicate a lognormal distribution.

$$f_{Tp|Uw,H_S}\left(t|u,h\right)=\frac{1}{\sqrt{2\pi}\sigma_{\ln(T_p)}t}\exp\left(-\frac{1}{2}\left(\frac{\ln(t)-\mu_{\ln(T_p)}}{\sigma_{\ln(T_p)}}\right)^2\right) \qquad (14)$$

where $\mu_{\ln(T_p)}$ and $\sigma_{\ln(T_p)}$ are the parameters in the conditional lognormal distribution, i.e. the mean value and standard deviation of ln(t) at each combination of wave-wind class. Unlike in Eq. (7), now the parameters in the lognormal distribution are functions of both H_s and U_w. According to the relationships:

$$\mu_{\ln(T_p)}=\ln\left[\frac{\mu_{T_p}}{\sqrt{1+\upsilon_{T_p}^2}}\right],\ \sigma_{\ln(T_p)}^2=\ln\left[\upsilon_{T_p}^2+1\right],\ \upsilon_{T_p}=\frac{\sigma_{T_p}}{\mu_{T_p}} \qquad (15)$$

μ_{T_p} and σ_{T_p} are the mean value and standard deviation of T_p. υ_{T_p} is the coefficient of variance (COV) .We need to fit μ_{T_p} and υ_{T_p} as functions of U_w and H_s to express the conditionality. Figure 8 shows the variation of the two parameters with H_s and U_w. In the figure, the wave-wind classes with limited number of data were excluded from the analysis to avoid large uncertainties.

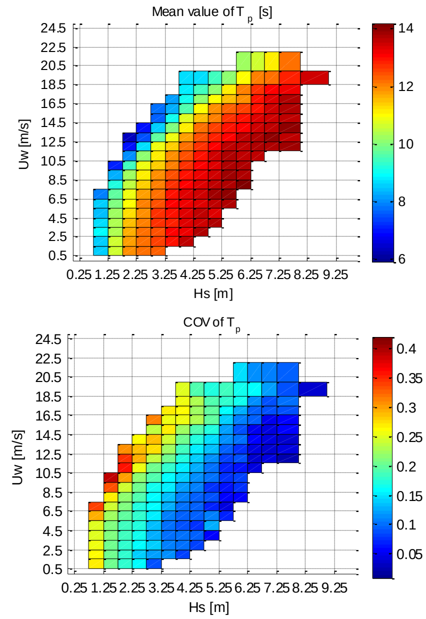

FIGURE 8. MEAN AND COV OF T_p FOR EACH WIND-WAVE CLASS (SITE 14)

It can be observed that the two parameters are dependent mainly on H_s, while they shift with the variation of wind speed. Based on this, the parameterization of T_p in the lognormal distribution could follow the methods suggested by Johannessen et al. [7]. The details of the method will not be given, but important equations are listed to explain the approach. The mean value of T_p can be modelled by the following equation.

$$\mu_{T_p}=\overline{T_p}\left(u,h\right)=\overline{T_p}\left(h\right)\cdot\left[1+\theta\left(\frac{u-\bar{u}(h)}{\bar{u}(h)}\right)^{\gamma}\right] \qquad (16)$$

where $\overline{T_p}(h)$ and $\bar{u}(h)$ are the expected spectral peak period and mean wind speed for a given value of H_s. The two expected values are fitted as a function of H_s:

$$\overline{T_p}\left(h\right)=e_1+e_2\cdot h^{e_3} \qquad (17)$$

$$\bar{u}\left(h\right)=f_1+f_2\cdot h^{f_3} \qquad (18)$$

The term $\left[1+\theta\left(\frac{u-\bar{u}(h)}{\bar{u}(h)}\right)^{\gamma}\right]$ adjusts the expected T_p according to whether the actual wind speed is above or below the expected wind speed for the particular significant wave height. In order to give reasonable values for θ and γ, Eq. (16) can be rewritten as,

$$\frac{\overline{T_p}\left(u,h\right)-\overline{T_p}\left(h\right)}{\overline{T_p}\left(h\right)}=\theta\left(\frac{u-\bar{u}(h)}{\bar{u}(h)}\right)^{\gamma} \qquad (19)$$

where $\frac{\overline{T_p}(u,h)-\overline{T_p}(h)}{\overline{T_p}(h)}$ and $\frac{u-\bar{u}(h)}{\bar{u}(h)}$ are the normalized period and wind speed, respectively. For each H_s class, the normalized period was plotted as a function of the normalized wind speed. Nearly linear relationships were observed for most H_s classes indicating γ is close to 1. A mean value of θ from all H_s classes is used for the slope in Eq. (16).

Moreover, the coefficient of variation can be assumed as a function of only H_s for simplification.

$$\upsilon_{T_p}(h)=k_1+k_2\cdot\exp(hk_3) \tag{20}$$

From above analysis, all the parameters for obtaining the lognormal distribution in Eq. (14) are calculated. Thus, the joint distribution modelled in Eq. (10) could be obtained.

It should be mentioned that the T_p data used in the joint distributions are the peak periods of the complete wave spectrums including both swell and wind sea components. T_p values from swell and wind sea are not analysed separately, which might not be physical when fitting conditional distribution of T_p. One possible way to improve the fitting method is to fit the T_p values from swell and wind sea spectrums individually. In this case, a more complicated model is needed to fit the data.

Distribution parameters and environmental contour surface

By fitting the raw data with analytical distributions, the parameters in the long-term joint distributions are estimated for the five selected sites, which are presented in Tables 3, 4 and 5 in Appendix A. The associated equations are Eqs. (4)-(20).

Based on the joint distribution, a contour surface with a return period of 50 years can be obtained. This is done by transforming the joint distribution into a non-physical space consisting of three independent standard Gaussian variables using Rosenblatt transformation [13]. The three variables are reflecting the marginal variability of U_w, conditional variability of H_s given U_w and conditional variability of T_p given U_w and H_s, respectively. In this space, all 50-year combinations of the variables will be located on a sphere with a radius, r, given by

$$\Phi(r)=1-\frac{1}{N_{50}} \tag{21}$$

N_{50} is the total number of one-hour sea state in 50 years. The 50-year contour surface of U_w, H_s and T_p can be obtained by transforming this sphere back to the physical parameter spaces.

The 3D 50-year contour surfaces for the five selected sites are shown in Figures 9-13 in Appendix B. In order to get readable values, the 2D contour lines of H_s and T_p for different levels of U_w are achieved from the contour surfaces and are also shown in the figures. For other values of U_w, interpolation might be applied to obtain the H_s-T_p contour lines. Each figure contains eight sub-figures. The top-left sub-figure is the 3D contour surface and the top-right one shows the condition on the contour surface corresponding to the maximum mean wind speed, and the following six sub-figures are contour lines of H_s and T_p for different levels of mean wind speed.

Moreover, two particular extreme conditions from the contour surface are given in Table 2. The first one corresponds to the condition with the maximum mean wind speed and the second one corresponds to the condition with the maximum significant wave height. For structures that are not sensitive to wave periods, it might be sufficient to consider the extreme conditions in Table 2 for ultimate load state analysis.

TABLE 2. ENVIRONMEANTAL CONDITIONS ON THE 50-YEAR CONTOUR SURFACES WITH MAXIMUM U_w OR MAXIMUM H_s

Condition	Parameter	Site 01	Site 03	Site 05	Site 14	Site 15
Condition with maximum U_w	U_w (*m/s*)	23.7	28.3	27.5	33.6	27.2
	H_s (*m*)	8.0	8.8	11.4	13.4	8.1
	T_p (*s*)	12.2	11.9	13.5	13.1	10.0
Condition with maximum H_s	U_w (*m/s*)	21.4	24.3	25.1	31.2	25.3
	H_s (*m*)	10.2	12.1	14.0	15.6	9.5
	T_p (*s*)	13.8	13.8	15.11	14.5	12.3

Simplified joint distribution of U_w, H_s and T_p

The process of obtaining the distribution of T_p conditionally on both H_s and U_w is very complicated following the methods described by Johannessen et al. [7]. It is not straightforward to find a reasonable relationship between distribution parameters and U_w. Moreover, the raw data indicate that the dependency of the distribution parameters for T_p on U_w is limited as seen from Figure 8. Hence, a simplified method is proposed that the distribution parameters for T_p are only dependent on H_s, which simplifies the joint PDF of U_w, H_s and T_p as,

$$f_{Uw,Hs,Tp}(u,h,t)\approx f_{Uw}(u)\cdot f_{Hs|Uw}(h|u)\cdot f_{Tp|Hs}(t|h) \tag{22}$$

The marginal distribution of U_w, conditional distribution of H_s for given U_w and the conditional distributuion of T_p for given H_s are all examined in the analysis above. As the conditional distribution of T_p is only dependent on H_s, the fitting of the lognormal parameters could be easily obtained. Following the simplified method, a contour surface can be also obtained and Figure 14 shows the contour surfaces from the simplified method for site 14. By comparing Figure 14 with the contour surface obtained from the complete methods in Figure 13, we can see that:

1) The T_p values at critical conditions which correspond to the largest H_s value for a given U_w level are almost the same from the two contours.

2) For larger T_p values, the corresponding H_s values are larger from the simplified method.

3) The shape of the contour lines for a given U_w level is skewed towards smaller T_p values for small H_s when taking U_w into consideration. The possible explanation is that the local wind increases the steepness of the wave, which results in smaller T_p value in the same H_s level. Because of this, the contours lines from the complete method cover broader range of

small T_p values compared with those from the simplified method.

Therefore, for structures which are not sensitive to small T_p values (normally less than 8s), the simplified method does not influence the determination of critical conditions for design, and gives larger H_s values for larger T_p value. However, if the structures are sensitive to T_p value, the complete method should be applied to get more accurate contour lines.

CONCLUSIONS

1) Environmental conditions at eighteen European offshore sites are given in the MARINA Platform project. It is observed that sites at the Atlantic area have more wave energy resources compared with those at the North Sea area, while the variations in the wind energy resource from area to area are not significant as compared to the variations in the wave energy resource. The extreme values of H_s are larger in the Atlantic area. During site selections, both energy resources and extreme conditions should be evaluated to maximize the power output and meanwhile reduce the potential costs of the combined wind and wave concepts. Five sites for concept design are selected from the eighteen sites considering these important factors as well as geographic conditions.

2) Long-term joint distributions of U_w, H_s and T_p, marginal distributions of U_w as well as joint distributions of H_s and T_p at five selected sites are presented. The long-term joint distribution can be applied to estimate the wind and wave power output from combined concepts, and to assess the fatigue damage. The marginal distributions of wind and wave can be used to estimate the wind and wave power separately. The parameters in the joint distributions are achieved by fitting hourly sampled data from 2001-2010 with analytical distributions. The data used in this paper are hindcast data generated from numerical model using assimilation techniques.

3) A simplified method is proposed to represent the long-term joint distributions of U_w, H_s and T_p by considering that the conditional distribution of T_p only depends on H_s. Comparisons are made between the simplified and the complete methods. The simplified method does not influence the determination of critical conditions for design, and will lead to larger H_s values for larger T_p values. For structures sensitive to the T_p, the complete method is recommended. In addition, improvements in fitting the conditional distribution of T_p could be made by examining wave periods from swell and wind sea components separately.

4) The 50-year contour surfaces for five selected sites are presented. From the contour surfaces, the 50-year extreme conditions could be selected. For different concepts, the most critical conditions may vary depending on the concept characteristics.

ACKNOWLEDGMENTS

The authors gratefully acknowledge the financial support from the European Commission through the 7th Framework Programme (MARINA Platform – Marine Renewable Integrated Application Platform, Grant Agreement 241402). The authors are also grateful to the Atmospheric Modeling and Weather Forecasting Group at NKUA for providing the hindcast data. The first author would like to thank Zhiyu Jiang from CeSOS, NTNU for valuable discussions.

REFERENCES

[1] Israel Martínez, Carlos López Pavón (2011) Deliverable D3.4: Recommended concepts for further documentation and analysis, Marine Renewable Integrated Application Platform, December 2011

[2] IEC (2005) Wind turbines – Part 1: Design requirements. IEC-61400-1. International Electrotechnical Commission.

[3] Winterstein, S. R., Ude, T. C., Cornell, C. A., Bjerager, P. and Haver, S. (1993) Environmental Parameters for Extreme Response: Inverse Form with Omission Factors. ICOSSAR-93, Innsbruck, Austria.

[4] Meling, T. S., Johannessen, K., Haver, S. and Larsen, K. (2000): Mooring Analysis of a Semi-Submersible by use of IFORM and Contour Surfaces, Proceedings of ETCE/OMAE2000 Joint Conference for the New Millennium, no. OMAE2000/osu oft-4141, February 14-17, 2000, New Orleans, LA, USA.

[5] DNV (2010): Recommended Practice - Environmental Conditions and Environmental Loads. DNV-RP-C205. Det Norske Veritas.

[6] Winterstein, S. R. and Engebretsen, K. (1998): Reliability-Based Prediction of Design Loads and Responses for Floating Ocean Structures. OMAE-1998, Lisbon, Portugal.

[7] Johannessen, K., Meling, T. S. and Haver, S. (2001): Joint Distribution for Wind and Waves in the Northern North Sea. ISOPE-2001, Stavanger, Norway.

[8] Cradden, L., Ingram, D., Davey, T. and Sofianos, S. (2010) Deliverable D2.1: Site assessment, Marine Renewable Integrated Application Platform, September 2010

[9] Galanis, G., Emmanouil, G., Chu, P. C. and Kallos, G. (2009): A new methodology for the extension of the impact of data assimilation on ocean wave prediction. Ocean Dynamics (2009) 59:523–535

[10] Emmanouil, G., Galanis, G. and Kallos, G. (2010): A new methodology for using buoy measurements in sea wave data assimilation. Ocean Dynamics (2010) 60:1205-1218

[11] Saulnier, J. B. (2012): Comparison of SKIRON wave model against *in situ* buoy measurements on SEM-REV, Marine Renewable Integrated Application Platform, November 2012

[12] Haver, S. (1980): Analysis of Uncertainties Related to the Stochastic Modelling of Ocean Waves. Ph.D. thesis, Norwegian Institute of Technology, Trondheim, Norway.

[13] Madsen, H. O., Krenk, S. and Lind, N. C. (1986): Methods of Structural Safety, Prentice-Hall, Inc., Englewood Cliffs, New Jersey, 1986.

APPENDIX A: DISTRIBUTION PARAMETERS AT FIVE SELECTED SITES

TABLE 3. PARAMETERS FOR THE MARGINAL DISTRIBUTIONS OF U_w $f_{Uw}(u)$

Parameter	Associated equation	Site No. 01	Site No. 03	Site No. 05	Site No. 14	Site No. 15
α_U	Eq. (4)	2.262	2.002	2.050	2.029	2.299
β_U	Eq. (4)	7.635	7.866	7.859	9.409	8.920

TABLE 4. PRAMETERS FOR THE JOINT DISTRIBUTION OF H_s AND T_P $f_{Hs,Tp}(h,t) = f_{Hs}(h) \cdot f_{Tp|Hs}(t|h)$

Distributions	Parameter	Associated equation	Site No. 01	Site No. 03	Site No.0 5	Site No. 14	Site No. 15
Marginal distribution of H_s	h_0	Eq. (6)	3.5	5.0	5.0	5.0	2.5
	μ_{LHM}	Eq. (6)	0.256	0.783	0.595	0.871	0.334
	σ_{LHM}	Eq. (6)	0.583	0.493	0.557	0.506	0.615
	α_{HM}	Eq. (6)	1.160	1.385	1.179	1.433	1.369
	β_{HM}	Eq. (6)	1.309	2.229	1.785	2.547	1.653
Conditional distribution of T_p for given H_s	c_1	Eq. (8)	1.900	2.008	2.004	1.886	1.587
	c_2	Eq. (8)	0.429	0.363	0.321	0.365	0.222
	c_3	Eq. (8)	0.272	0.295	0.332	0.312	0.674
	d_1	Eq. (9)	0.001	0.001	0.001	0.001	0.008
	d_2	Eq. (9)	0.205	0.068	0.103	0.105	0.227
	d_3	Eq. (9)	-0.487	-0.300	-0.285	-0.264	-0.956

TABLE 5. PARAMETERS FOR THE JOINT DISTRIBUTION OF U_w, H_s ANDT_p $f_{Uw,Hs,Tp}(u,h,t) = f_{Uw}(u) \cdot f_{Hs|Uw}(h|u) \cdot f_{Tp|Uw,Hs}(t|u,h)$

Distributions	Parameter	Associated equation	Site No. 01	Site No. 03	Site No. 05	Site No. 14	Site No. 15
Marginal U_w	α_U	Eq. (4)	2.262	2.002	2.050	2.029	2.299
	β_U	Eq. (4)	7.635	7.866	7.859	9.409	8.920
Conditional H_s for given U_w	a_1	Eq. (12)	1.894	1.643	2.044	2.136	1.755
	a_2	Eq. (12)	0.012	0.093	0.034	0.013	0.184
	a_3	Eq. (12)	1.741	1.000	1.375	1.709	1.000
	b_1	Eq. (13)	0.929	1.969	1.323	1.816	0.534
	b_2	Eq. (13)	0.024	0.031	0.032	0.024	0.070
	b_3	Eq. (13)	1.827	1.644	1.757	1.787	1.435
Conditional T_p for given U_w and H_s	θ	Eq. (16)	-0.268	-0.143	-0.233	-0.255	-0.477
	γ	Eq. (16)	1.0	1.0	1.0	1.0	1.0
	e_1	Eq. (17)	5.0	5.0	8.0	8.0	5.563
	e_2	Eq. (17)	5.883	5.970	2.600	1.938	0.798
	e_3	Eq. (17)	0.201	0.223	0.409	0.486	1.0
	f_1	Eq. (18)	2.0	1.0	1.8	2.5	3.5
	f_2	Eq. (18)	3.947	4.055	3.478	3.001	3.592
	f_3	Eq. (18)	0.620	0.466	0.667	0.745	0.735
	k_1	Eq. (20)	-0.002	0.030	0.002	-0.001	0.050
	k_2	Eq. (20)	0.341	0.234	0.298	0.316	0.388
	k_3	Eq. (20)	-0.186	-0.221	-0.166	-0.145	-0.321

APPENDIX B: FIFTY-YEAR CONTOUR SURFACES AT FIVE SELECTED SITES

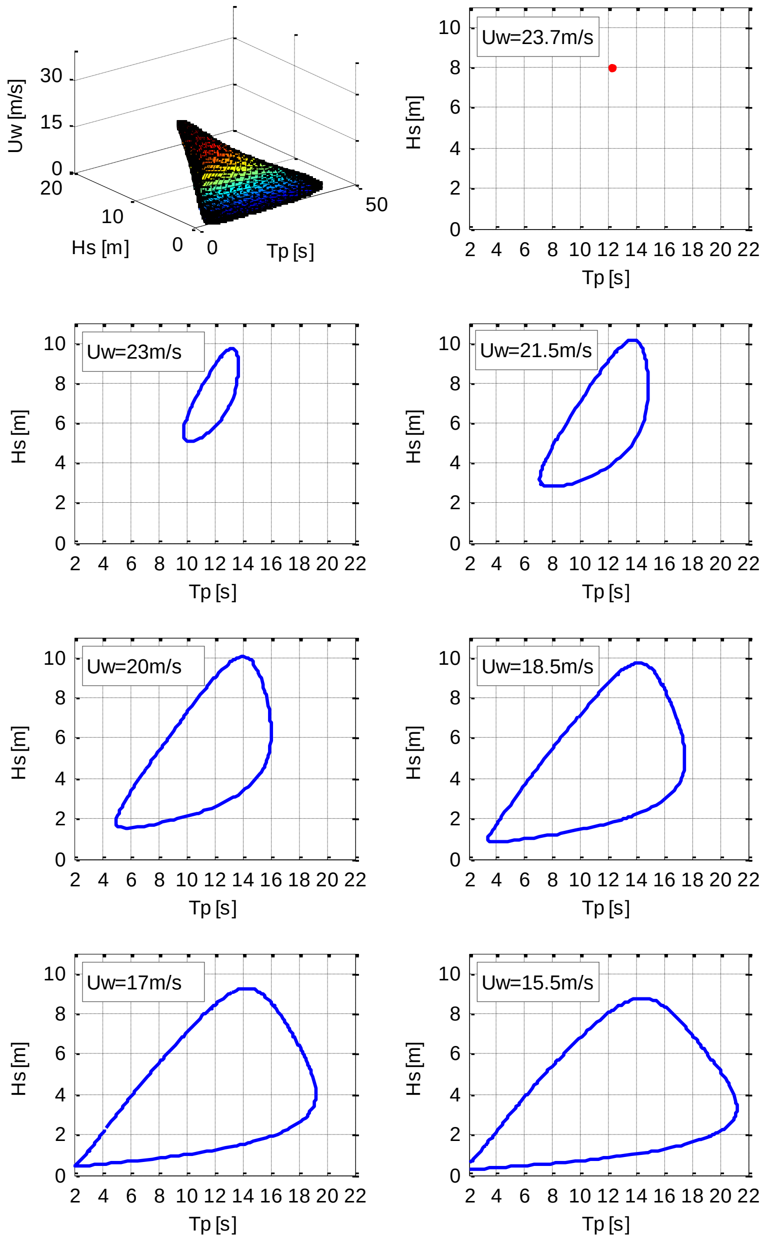

FIGURE 9. FIFTY-YEAR CONTOUR SURFACE FOR SITE 01 (COMPLETE METHOD)

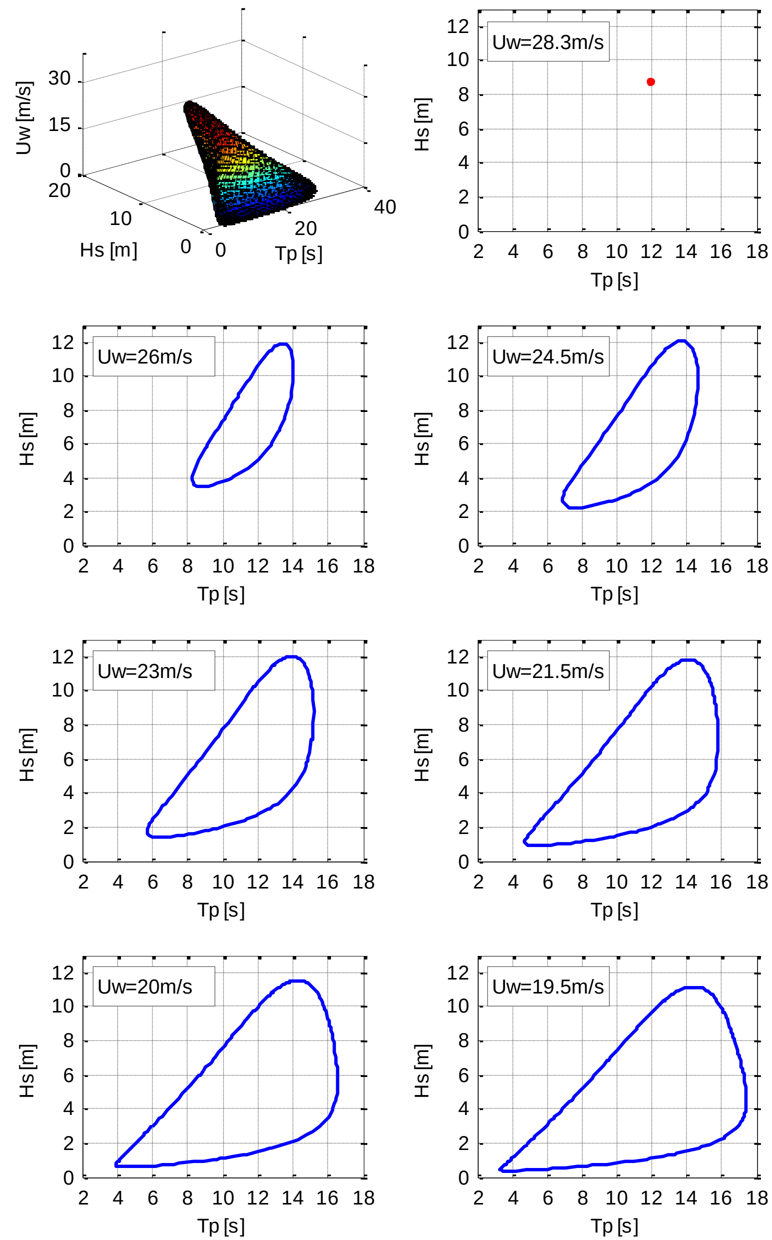

FIGURE 10. FIFTY-YEAR CONTOUR SURFACE FOR SITE 03 (COMPLETE METHOD)

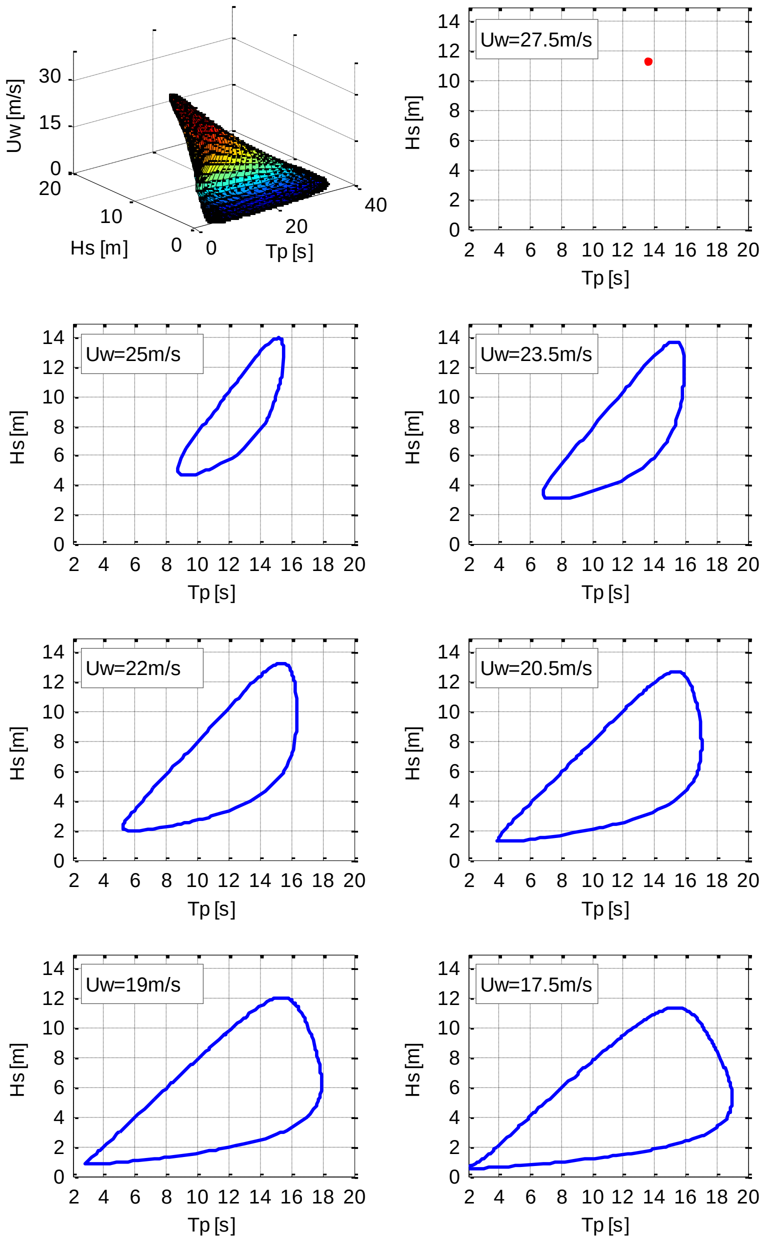

FIGURE 11. FIFTY-YEAR CONTOUR SURFACE FOR SITE 05 (COMPLETE METHOD)

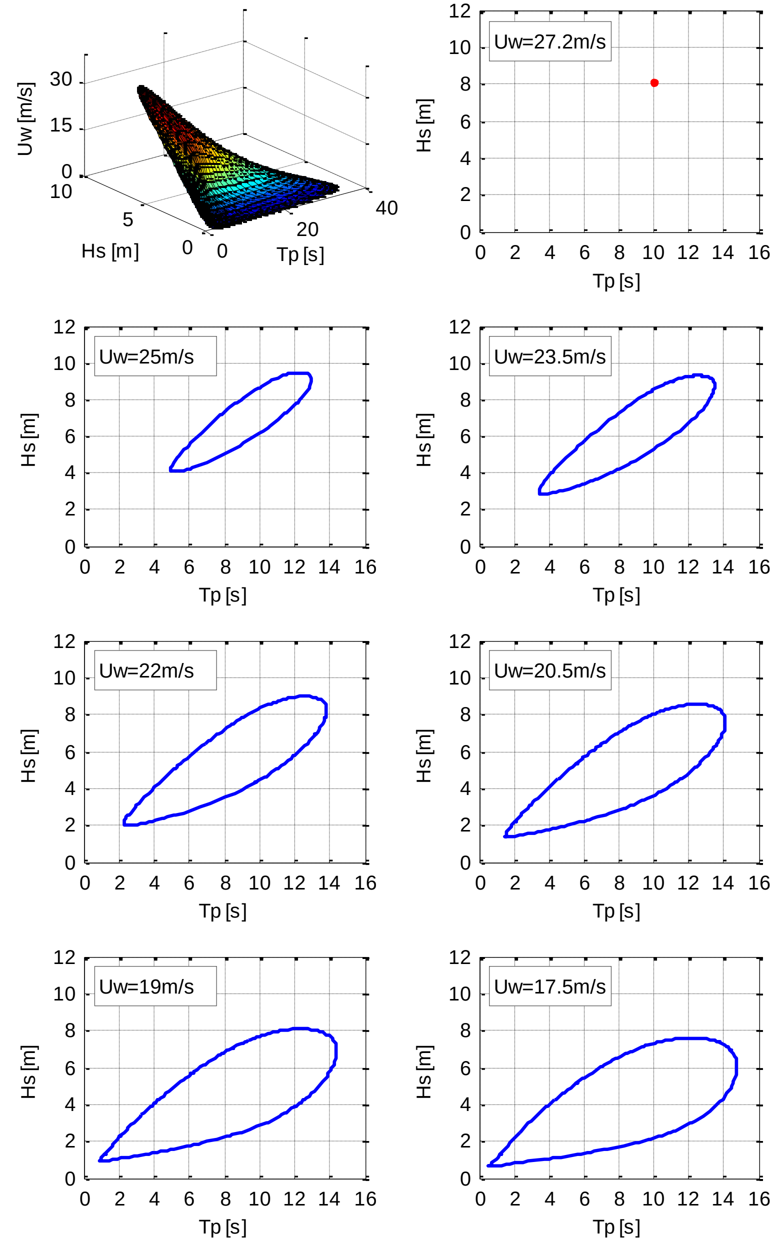

FIGURE 12. FIFTY-YEAR CONTOUR SURFACE FOR SITE 15 (COMPLETE METHOD)

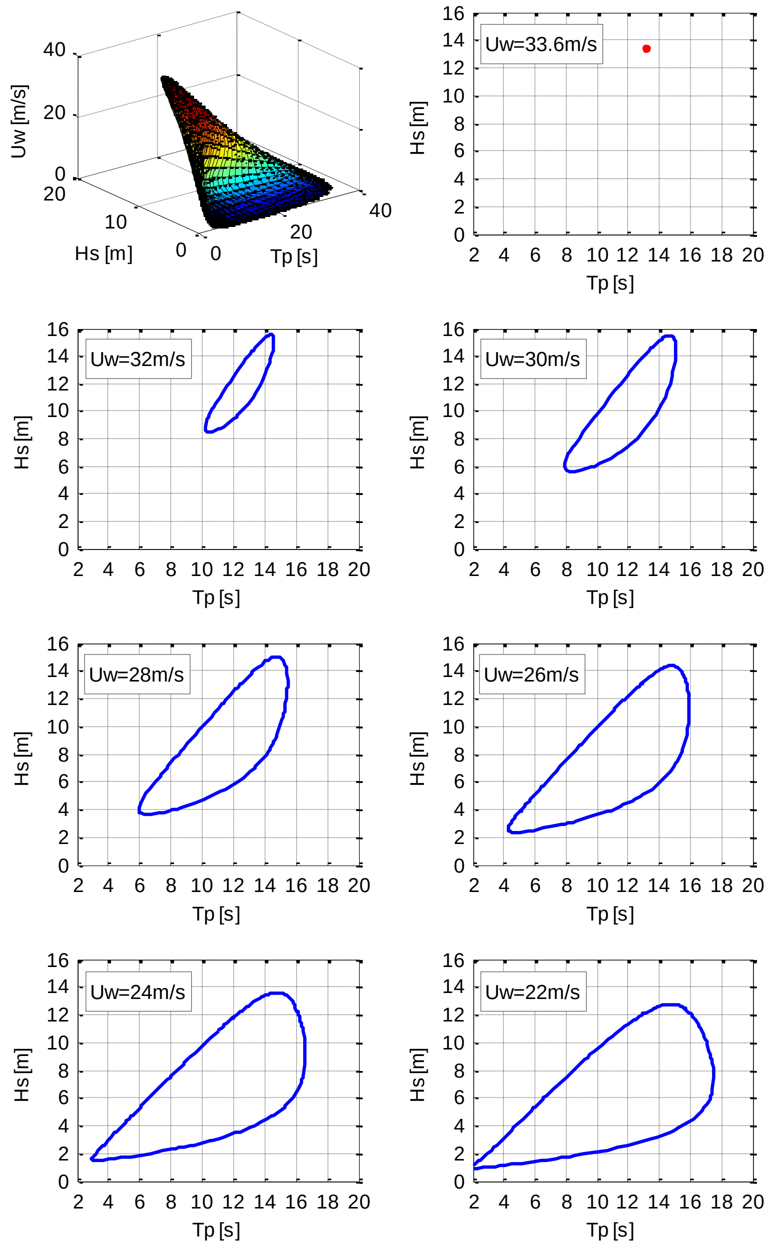

FIGURE 13. FIFTY-YEAR CONTOUR SURFACE FOR SITE 14 (COMPLETE METHOD)

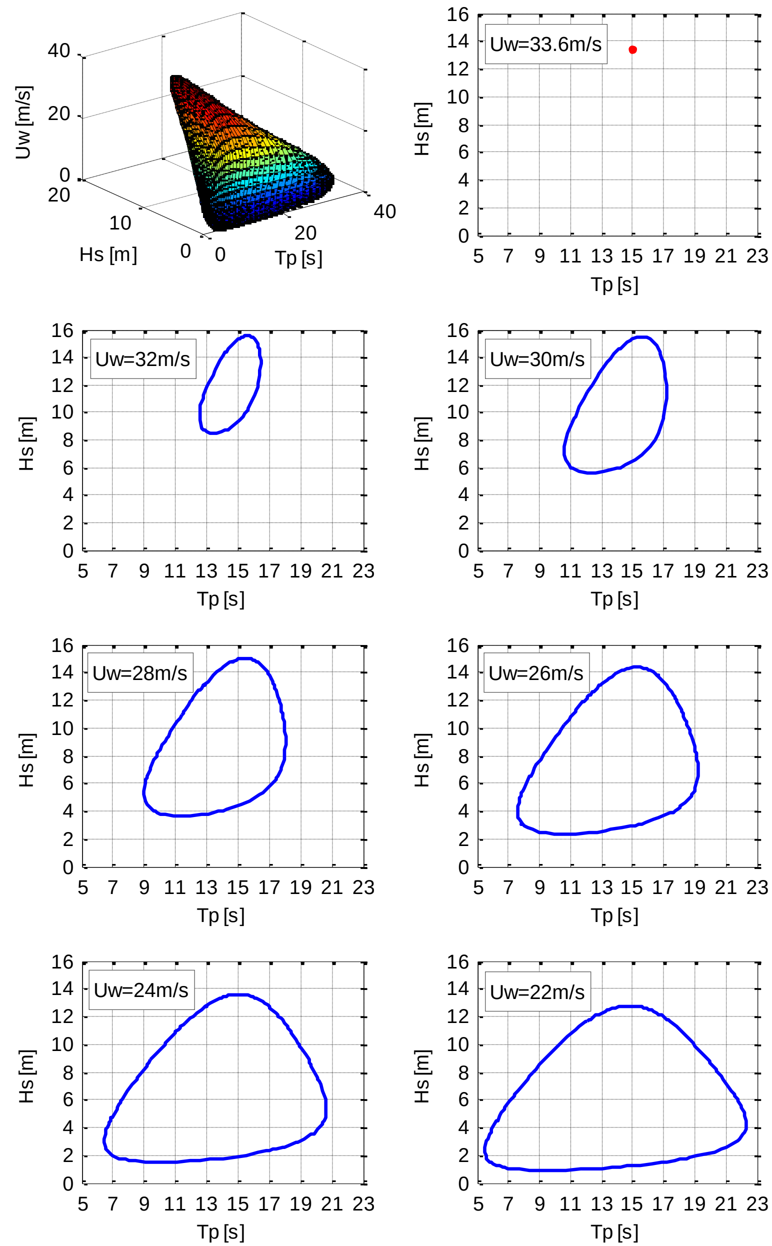

FIGURE 14. FIFTY-YEAR CONTOUR SURFACE FOR SITE 14 (SIMPLIFIED METHOD)